



Ecophysiological plasticity of Amazonian trees to long-term drought

Tomas Ferreira Domingues¹ · Jean Pierre Henry Balbaud Ometto² · Daniel C. Nepstad³ · Paulo M. Brando^{4,5} · Luiz Antonio Martinelli⁶ · James R. Ehleringer⁷

Received: 20 September 2017 / Accepted: 5 June 2018 / Published online: 28 June 2018
© Springer-Verlag GmbH Germany, part of Springer Nature 2018

Abstract

Episodic multi-year droughts fundamentally alter the dynamics, functioning, and structure of Amazonian forests. However, the capacity of individual plant species to withstand intense drought regimes remains unclear. Here, we evaluated ecophysiological responses from a forest community where we sampled 83 woody plant species during 5 years of experimental drought (throughfall exclusion) in an eastern Amazonian *terra firme* forest. Overall, the experimental drought resulted in shifts of some, but not all, leaf traits related to photosynthetic carbon uptake and intrinsic water-use efficiency. Leaf $\delta^{13}\text{C}$ values increased by 2–3‰ within the canopy, consistent with increased diffusional constraints on photosynthesis. Decreased leaf C:N ratios were also observed, consistent with lower investments in leaf structure. However, no statistically significant treatment effects on leaf nitrogen content were observed, consistent with a lack of acclimation in photosynthetic capacity or increased production of nitrogen-based secondary metabolites. The results of our study provide evidence of robust acclimation potential to drought intensification in the diverse flora of an Amazonian forest community. The results reveals considerable ability of several species to respond to intense drought and challenge commonly held perspectives that this flora has attained limited adaptive plasticity because of a long evolutionary history in a favorable and stable climate.

Keywords Global change · Stable isotope · Nutrient · Primary productivity · Functional group

Communicated by Russell K. Monson.

Electronic supplementary material The online version of this article (<https://doi.org/10.1007/s00442-018-4195-2>) contains supplementary material, which is available to authorized users.

✉ Tomas Ferreira Domingues
tdomingu@gmail.com

¹ Faculdade de Filosofia, Ciências e Letras (FFCLRP-USP),
Ribeirão Preto, SP, Brazil

² Instituto Nacional de Pesquisas Espaciais (INPE),
São José dos Campos, SP, Brazil

³ Earth Innovation Institute, San Francisco, CA, USA

⁴ Woods Hole Research Center, Falmouth, MA, USA

⁵ Instituto de Pesquisa Ambiental da Amazônia (IPAM),
Belém, PA, Brazil

⁶ Centro de Energia Nuclear na Agricultura (CENA-USP),
Piracicaba, SP, Brazil

⁷ University of Utah, Salt Lake City, UT, USA

Introduction

The negative impacts of El Niño-related droughts on productivity of wet, tropical rain forests today are well known, but the mechanistic basis for these responses are less well understood (Cox et al. 2004; Huntingford et al. 2013; Rowland et al. 2015). Several lines of evidence suggest that multi-year droughts will become more frequent, more intense, and more expansive as climate and tropical land-use changes persist (Duffy et al. 2015). The response of tropical forest trees to a shift in drought regimes remains poorly understood and beyond our current projection capabilities (Nepstad et al. 2007), despite the potentially large ecological and socio-economic impacts capable of altering regional carbon balance and biodiversity. Understanding of the mechanisms by which droughts influence the capacity of tropical forest trees to assimilate carbon and use water would reduce uncertainties in model projections.

Direct effects of drought on photosynthesis influence carbon fluxes with cascading direct and indirect influences on mortality, ecosystem structure, biogeochemical cycling, and community dynamics (Feldpausch et al. 2017). Amazonian

tree species exhibit features to avoid or cope with droughts, while sustaining photosynthetic activity, including hydraulic lift, photosynthetic acclimation, and leaf shedding (Oliveira et al. 2005). The prospect of more frequent droughts could increase selection towards greater intrinsic water-use efficiency (Cernusak et al. 2009). By conventional wisdom, such shifts would signify a novel evolutionary landscape, given the commonly accepted perspective of the wet tropical climates and associated communities as relatively stable.

Much of our current understanding of forest responses to drought is derived from simulations of coupled earth system and climate models (Andreae et al. 2004; Boisier et al. 2015; Cox et al. 2004, 2013; Marengo et al. 2010; Silva-Dias et al. 2002). These simulations forecast increased warming and greater drying over the Amazon Basin that could drive large-scale reductions in regional biomass. The processes in these models that drive projections of decreased biomass loss relate to reductions in photosynthesis triggered by stress-induced biosphere–atmosphere feedbacks, limited drought acclimation potential, and shifts toward less favorable tree carbon balances. However, these future carbon balance projections are modulated by CO₂ fertilization (Norby et al. 2016).

To reduce the uncertainties associated with drought-induced changes in the functioning of Amazonian forests, we investigated how a tropical forest ecosystem responded to long-term experimental soil drying (referred to as *Seca Floresta*) (Nepstad et al. 2002). In particular, we evaluated progressive drought-induced impacts on foliar carbon, nitrogen, and stable isotope ratios, which represent proxies of ecophysiological gas-exchange processes. Large-scale, long-term field experiments, such as *Seca Floresta*, represent an important opportunity to identify how plants respond to persistent shortages in soil moisture at the community scale. We expected that experimental drought would reveal physiological responses typical of earlier studies of general plant responses to chronic water stress. As a first-order prediction, we hypothesized that Amazonian trees would show (1) decreased stomatal conductances associated with declines in water loss from transpiration, (2) increased leaf sclerophyll that contribute to reduced mesophyll conductance to CO₂ assimilation (Flexas et al. 2008), and (3) decreased evaporative canopy surface area driven by increased leaf shedding. Trait trade-off conflicts might exist for some of these expected responses. Both decreased diffusional conductance and reduced leaf area impact tree crown water loss, but also constrain photosynthetic carbon uptake. At some point, a trade-off dilemma is reached where species that do not restrict photosynthesis during drought stress attain higher carbon uptake but risk catastrophic xylem embolism (Anderegg et al. 2015; Sperry 2000) and death by “thirst” (Rowland et al. 2015). At the other trade-off extreme, if plants reduce photosynthesis to avoid water loss, plants

will ultimately incur a negative carbon balance and possible death by carbon starvation, if respiratory carbon losses become larger than photosynthetic carbon uptake (McDowell et al. 2008). While this strategy might be advantageous during short drought events, it might become fatal during intense, prolonged drought events.

The primary focus of the present study is how tropical ‘wet’ rain forest woody species respond to decreased soil moisture during persistent drought. Bearing in mind that, by conventional wisdom, tropical rain forest trees are both adapted to predictable water availability and display limited photosynthetic plasticity, the following specific questions were addressed: (1) To what degree does interspecific diversity exist in the physiological responses of wet tropical forest trees to persistent drought? (2) How much ecophysiological plasticity is evident in traits associated with leaf carbon balance during a prolonged drought? (3) If plasticity is present, does it move traits of the community, as a whole, toward a more robust physiological state capable of utilizing limited water more efficiently to assimilate atmospheric CO₂. The answers to these questions will advance our understanding of the processes that must be included in process-based modeling of tropical forest carbon and water cycling to accurately predict future responses to a drier tropical climate.

Methods

Site description

The study area was located at FLONA Tapajós (Tapajós National Forest), denominated “km 67” site, south of the city of Santarém, Pará, Brazil (2°26′35″S; 54°42′30″W). Established as a national forest in 1974, the area encompasses approximately 400,000 ha and consists of dense evergreen upland (*terra-firme*) tropical vegetation, with high productivity maintained by deep root systems through dry periods (Nepstad et al. 1994). The annual precipitation averages 2100 mm, meaning that this system represents a below average portion of the wetness spectrum for Amazonian vegetation. The sampling was carried out within the through-fall exclusion experiment, located at 2.8978S, 54.9528W (*SECA Floresta*), which consisted of two structurally and floristically similar 1 ha plots, as described in Nepstad et al. (2007). The plots refer to an ‘exclusion plot’ (treatment) and a ‘control plot’. The exclusion of precipitation at the treatment plot, achieved by installation of plastic panels placed at the understory, diverted approximately 40% of total “wet season” rainfall, from January 2000 to December 2004 (Nepstad et al. 2007; Brando et al. 2008). During the 5-month dry season (July–November), the plastic panels were removed and dry season precipitation was not excluded. The soils of this site are deeply weathered oxisols (Hapludox), with the water

table at 100 m bellow the soil surface; high clay content (60–80%), low pH (4.0–4.3) and low nutrient.

Sampling

From March 1999 until October 2004, 1222 leaf samples from different tree and liana species were collected from the two study plots. After averaging replicated samples when more than one leaf were collected during the same month, from the same individual, and at the same height within the canopy, 1044 data points were used for statistical analyses (Supplementary Material). The dataset is represented by 83 botanically identified plant species of trees and lianas from 192 different individual plants.

Analytical technique

Leaf samples were dried at 65 °C to a constant mass and ground to a fine powder. Subsamples (1–2 mg) were placed in tin capsules, weighed, and combusted in an elemental analyser (Carla Erba) coupled with an isotope ratio mass spectrometer (IRMS Delta plus, Finnigan MAT, Sao Jose, CA, USA), operating in continuous flow mode at the stable isotope ratio facility at CENA-USP. Stable isotope ratios ($\delta^{13}\text{C}$, $\delta^{15}\text{N}$) and elemental contents for carbon and nitrogen (C%, N%) were then obtained. Isotopic data were expressed with the “delta” notation ($\delta^{13}\text{C}$, $\delta^{15}\text{N}$) and per mil (‰) as described in Eq. (1):

$$\delta = \left\{ \frac{R_{\text{sample}} - R_{\text{standard}}}{R_{\text{standard}}} \right\} \times 1000, \quad (1)$$

where R_{sample} and R_{standard} are the ratio $^{13}\text{C}:^{12}\text{C}$ or the ratio $^{15}\text{N}:^{14}\text{N}$ of the sample and standard, respectively. Standards for carbon and nitrogen are PDB and air, respectively. Results are expressed on the international carbon (V-PDB) and nitrogen (AIR) scales.

Statistical analysis

To test for differences between the control and exclusion plots regarding foliar $\delta^{13}\text{C}$, $\delta^{15}\text{N}$, N concentration and C:N ratio, we pooled data from each sampling, further we grouped the foliar data according to canopy strata: understory, lower canopy, upper canopy, top canopy. The data are presented in Table 1 of the Supplementary Material (SM). Using this dataset we applied general linear mixing models (GLMMs), considering as fixed categorical variables the two plots (control and exclusion) and canopy strata, and as fixed continuous variable, we used the timespan since the beginning of the experiment (Table 2 of Supplementary Material). We consider timespan up to 60 months, because after that data for the control plot are not available.

For those parameters that were statistically different in the interaction plot \times canopy \times timespan, and using again data from Table 1 (Supplementary Material), we fit linear regressions between the leaf-parameter pooled data and timespan, expressed in months since the beginning of the exclusion experiment, for each canopy strata independently. Linear regressions were tested for statistical significance. Differences were considered significant at a probability level of 95% ($p < 0.05$). All tests were run in the STATISTICA13 software.

Results

Only $\delta^{13}\text{C}$ was significantly different between plots, considering interactions with canopy and time span since the beginning of the experiment. Accordingly, we fit linear regressions between foliar $\delta^{13}\text{C}$ vs. time span by canopy strata. We observed in the control plot a general tendency of increasing foliar $\delta^{13}\text{C}$ values with time (Fig. 1a). However, this trend was only significant for the understory and the upper canopy (Table 1). On the other hand, in the exclusion plot, all canopy strata showed a significant increase of $\delta^{13}\text{C}$ values in relation to time span since the beginning of the experiment (Fig. 1b). The slopes of the regression models ($\delta^{13}\text{C}$ vs. time) in the exclusion plot increased progressively from the understory to the top of the canopy (Table 2), indicating a gradient in responsiveness within the canopy. At the same time, intercept values also increased along the canopy (Table 2), probably due to the “canopy effect” (higher fraction of respired CO_2 fixation lower in the canopy profile, associated with lower light levels). This canopy effect can also be observed when the average foliar $\delta^{13}\text{C}$ values are plotted against canopy strata (Fig. 2a). In both plots, the increase in $\delta^{13}\text{C}$ along the canopy was very similar, and approximately 6‰ in magnitude from the understory to the canopy top.

It is important to note that in the exclusion plot the increasing trend in $\delta^{13}\text{C}$ values with time lasted only up to 60 months (Fig. 1b). After that, $\delta^{13}\text{C}$ values had no clear trends (top canopy) or even a decreasing trend for the other canopy strata (Fig. 1b). Unfortunately, the control plot was

Table 1 Statistical values of the regressions relating foliar $\delta^{13}\text{C}$ and time (expressed in months) at four different canopy heights in the control plot since the beginning of the exclusion experiment

	Intercept	Slope	r^2	F	P
Understory	−36.36	0.032	0.58	12.11	0.010
Lower	−33.71	0.023	0.08	2.38	0.16
Upper	−32.91	0.032	0.36	9.51	0.0081
Top	−30.24	0.019	0.11	2.79	0.12

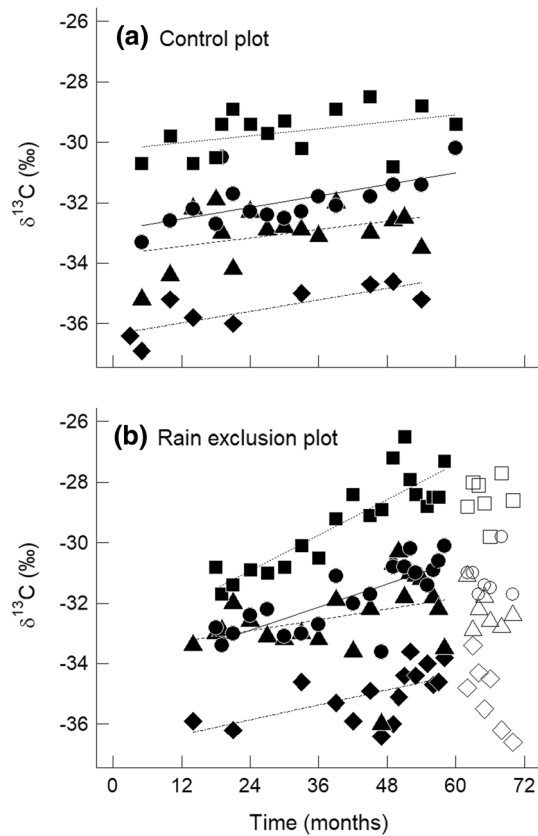


Fig. 1 Foliar $\delta^{13}\text{C}$ versus time since the beginning of the exclusion experiment. Understory (filled diamond), lower canopy (filled triangle), upper canopy (filled circle) and top canopy (filled square). Open symbols in **b** represent data from after 60 months, when no matching samples were taken from the control plot. Lines represent linear regression fits between foliar $\delta^{13}\text{C}$ and time up to 60 months. Statistical values of these regressions are presented in Tables 1 and 2

Table 2 Statistical values of the regressions relating foliar $\delta^{13}\text{C}$ and time (expressed in months) at four different canopy heights in the exclusion plot since the beginning of the exclusion experiment

	Intercept	Slope	r^2	F	P
Understory	−36.84	0.041	0.31	7.75	0.015
Lower	−33.63	0.030	0.07	2.66	0.12
Upper	−34.43	0.064	0.59	27.95	0.000050
Top	−33.29	0.098	0.77	66.35	0.00000019

not sampled after 60 months and one cannot be sure if the same trend would also be observed for the control plot vegetation (Fig. 1a).

Foliar $\delta^{15}\text{N}$, N concentration and C:N ratio data were also pooled by sampling date, and canopy strata, like for foliar $\delta^{13}\text{C}$. However, none of them had a significant difference considering plot \times canopy \times time span interactions (Table 2 Supplementary Material). As no specific trend

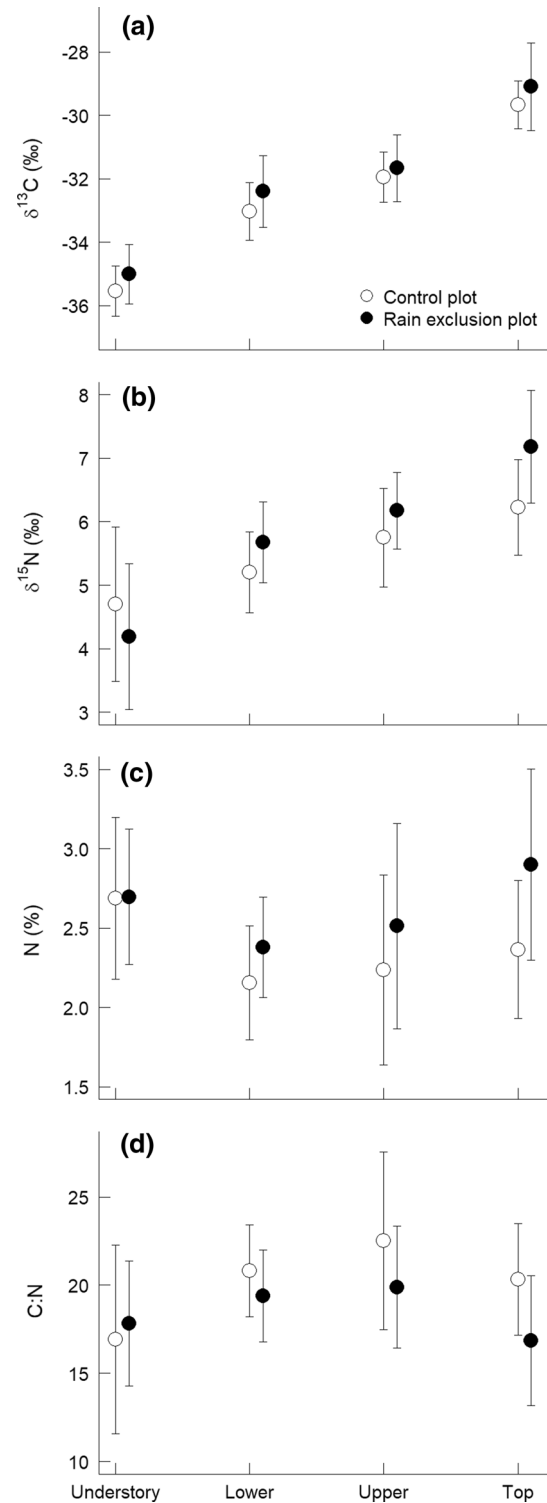


Fig. 2 Variability of foliar **a** $\delta^{13}\text{C}$, **b** $\delta^{15}\text{N}$, **c** N concentration, and **d** C:N ratio through the canopy for 60 months following the beginning of the exclusion experiment. Exclusion plot (filled circle) and control plot (open circle). Bars refer to standard deviation

was detected with timespan for these parameters we just described the temporal variability of these parameters. First, $\delta^{15}\text{N}$ increased up to 20 months after the beginning of the experiment, decreasing from 20 to 48 months, and increasing again until the end of our sampling (Fig. 3). It is unlikely that such time-variability was caused by rain exclusion, since in both plots the variability was similar in pattern. After 48 months, toward the end of the experiment, an increase in variance was observed for $\delta^{15}\text{N}$ values at the exclusion plot, especially in the top canopy stratum (Fig. 3b).

An important trend observed in both plots was an increase of foliar $\delta^{15}\text{N}$ values near the top of the canopy (Fig. 2b). In the control plot, this increase was approximately 1.5‰ between the understory and the top of the canopy, and in the exclusion plot was approximately 3‰ (Fig. 2b).

The foliar N concentration in the exclusion plot, slight decrease from the beginning of our observations to approximately 40 months, and then increase again, toward the end of the sampling period (Fig. 4). After this period (40 months), the observed variance increased in the exclusion plot (Fig. 4b). Along the canopy, N concentration varied in a

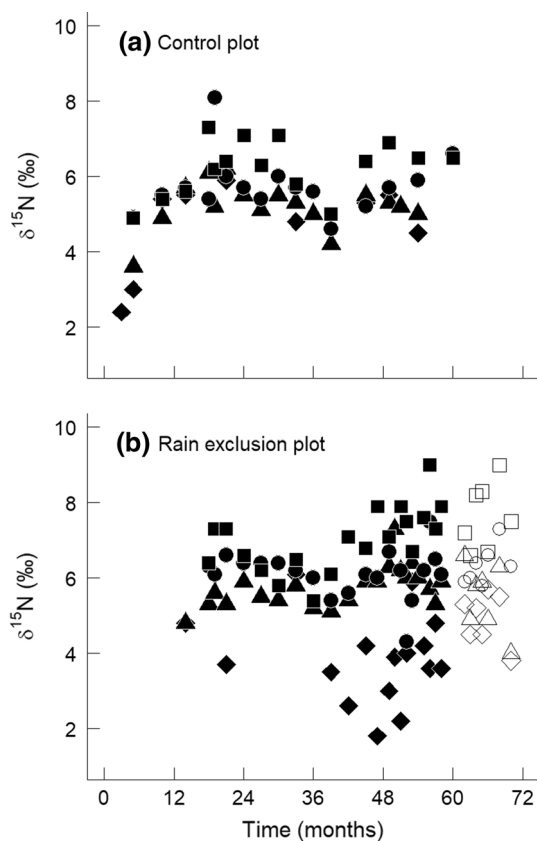


Fig. 3 Foliar $\delta^{15}\text{N}$ versus time since the beginning of the exclusion experiment. Understory (filled diamond), lower canopy (filled triangle), upper canopy (filled circle) and top canopy (filled square). Open symbols in **b** represent data from after 60 months, when no matching samples were taken from the control plot

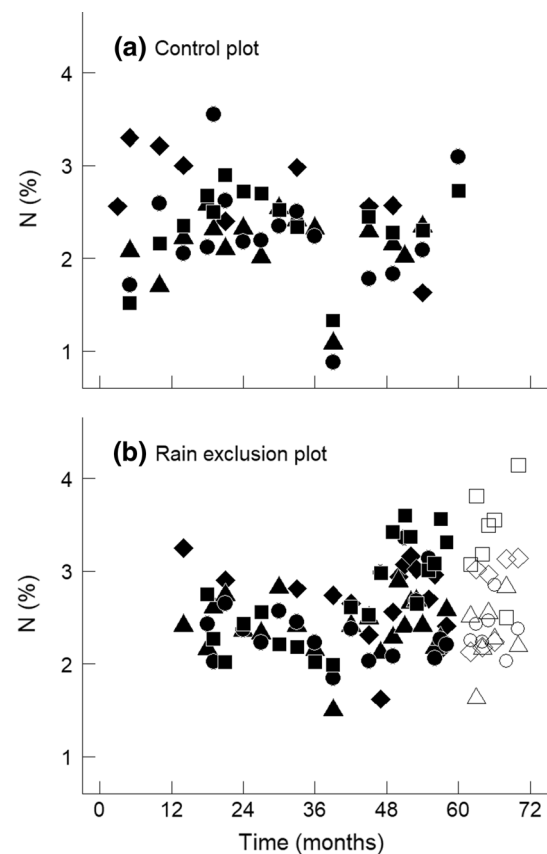


Fig. 4 Foliar N concentration versus time since the beginning of the exclusion experiment. Understory (filled diamond), lower canopy (filled triangle), upper canopy (filled circle) and top canopy (filled square). Open symbols in **b** represent data from after 60 months, when no matching samples were taken from the control plot

similar way in both plots (Fig. 2c). Nitrogen concentrations were higher in the understory and in the top of the canopy in comparison with the middle strata (Fig. 2c).

Foliar C:N ratio followed N concentration without any specific trend during the experiment (Fig. 5). Along the canopy, the major difference was lower C:N ratios in the understory than in the upper canopy (Fig. 5b).

Discussion

Interspecific diversity in drought responses

This study was based on repeated sampling of trees at both control and rain exclusion plots. Obviously but important, only surviving trees were sampled over the entire simulated drought time. From these observations, it is clear that not all tree species responded the same to drought. Trait variation through time indicated high variability in physiological responses. Complicating a simple interpretation is that

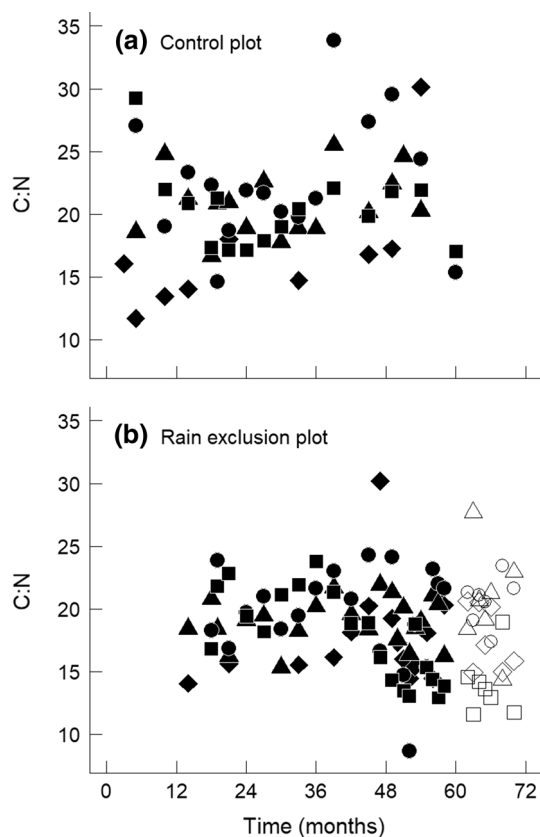


Fig. 5 Foliar C:N ratio versus time since the beginning of the exclusion experiment. Understory (filled diamond), lower canopy (filled triangle), upper canopy (filled circle) and top canopy (filled square). Open symbols in **b** represent data from after 60 months, when no matching samples were taken from the control plot

responses can be difficult to interpret as individual trees differed in canopy position, age, possibly in the extent of stored carbon reserves, and possibly in the degree to which mobilization of carbon reserves into new leaf construction was possible. While some tree species responded quickly to the drought, others exhibited delayed and differential responses. Thus, at the community level, a large number of Amazonian tree species were able to cope with a prolonged drought.

Intrinsic water-use efficiency reflects a balance between the supply of carbon dioxide through the stomata and its consumption in photosynthesis. Reductions in stomatal conductance reduce both photosynthetic and transpiration rates. It is well known that intrinsic water-use efficiency can be measured with leaf $\delta^{13}\text{C}$ values, which reflect a time-integrated measure (Farquhar et al. 1989). In the Seca Floresta study, we observed an increase in foliar $\delta^{13}\text{C}$ values during the imposed drought in the exclusion plot across different canopy strata. After 60 months, an apparently new state was reached where leaf $\delta^{13}\text{C}$ values did not increase further in those trees surviving the drought, suggesting that these trees had attained their highest intrinsic water-use efficiency

values. Decreased soil water volumetric content (WVC) at the exclusion plot (Brando et al. 2008) was most likely the driving force behind the increase of foliar $\delta^{13}\text{C}$ values. Decreased wood productivity reported for the exclusion plot (Brando et al. 2008) corroborated this hypothesis. Although, other processes could also have contributed to the decline in forest growth, such as a decrease in leaf area index (Brando et al. 2008) and increases in autotrophic respiration (Rowland et al. 2015), it seems likely that greater intrinsic water-use efficiencies were also contributing factors.

Ecophysiological plasticity is evident in traits associated with leaf carbon balance during a prolonged drought

Stable carbon isotope provides us with a tool to investigate ecosystem processes during drought. Here we observed that drought resulted in significant increases in leaf $\delta^{13}\text{C}$ values, and two mechanisms might also have contributed to resulting leaf $\delta^{13}\text{C}$ values. First, the use of stored carbon fixed prior to the onset of the rain exclusion by trees could have diluted leaf $\delta^{13}\text{C}$ values as new leaves were produced through the extended drought period. Second, decreases in canopy leaf area in response to drought (either by leaf shedding or even mortality of trees) might have reduced the rates of soil moisture declines, promoting improved leaf water potentials and consequently reducing stomatal limitation to photosynthesis, although lower leaf area can also lead to decreased isotopic discrimination as a result of more light reaching the canopy environment. Therefore, differences in the proportion of deciduousness trees among control and drought treatment sites could hinder direct inter-site comparisons. We have no evidence to evaluate this possibility.

The trend of increasing foliar $\delta^{13}\text{C}$ observed with long-term drought represents the mean physiological response of many species. These results contrast with a lack of responses of tropical tree species to normal dry season, suggested in Domingues et al. (2013), when a modest set of species was investigated at a nearby site. This apparent disagreement highlights the fact that the vegetation may be adapted to typical seasonal variations in water availability, and that only extended drought within the Tapajós region climate is sufficient to trigger increases in intrinsic water-use efficiency. Results from a similar rain exclusion experiment at a Caxiuanã forest (ongoing since 2001) detected no significant changes in leaf photosynthetic capacity between treatments indicating no compensating mechanism that could boost carbon uptake under lower stomatal conductance (Rowland et al. 2015).

We also asked how much ecophysiological plasticity is evident in traits associated with leaf carbon balance during a prolonged drought by examining changes in leaf $\delta^{15}\text{N}$, which has been used as a proxy of N availability (Högberg

et al. 1995), and foliar carbon to nitrogen ratios, and nitrogen contents as a proxy for photosynthetic capacity.

Overall, foliar $\delta^{15}\text{N}$ values were minimal and similar to other studies conducted in the same area (Ometto et al. 2006; Nardoto et al. 2014). Differences in $\delta^{15}\text{N}$ between control and exclusion plots were restricted to only lower canopy vegetation and showed no significant trend over time (Figs. 2b, 3). The increase in foliar $\delta^{15}\text{N}$ values with canopy height found here was also reported for an independent dataset from the Flona-Tapajós area (Ometto et al. 2006). In contrast, understory changes in $\delta^{15}\text{N}$ values were not observed in forests near Manaus and in the State of Rondônia (Ometto et al. 2006), tropical forests of Africa (Blumenthal et al. 2016), or tropical forests of South Asia (Roberts et al. 2017). One possible explanation for the observed $\delta^{15}\text{N}$ trend could be differential volatilization rates of nitrogen containing compounds from leaves along the canopy (Farquhar et al. 1979).

The differences in leaf N concentrations between control and exclusion plots were subtle and without clear trends, suggesting no appreciable changes in photosynthetic capacity over time. Interestingly, Carswell et al. (2000) found a similar non-significant trend in a *terra-firme* forest near Manaus, in Central Amazon.

Foliar N concentrations reported here (average $24.1 \pm 7.8 \text{ mg g}^{-1}$) are similar in range to concentrations previously reported for nearby areas (Domingues et al. 2007; Ometto et al. 2006; Quesada et al. 2010). These values also similar to the mean found among more than 1000 trees distributed over 65 rainforest plots in the Amazon basin (Fyllas et al. 2009).

The foliar C:N ratios of trees in the exclusion plot were significantly lower compared to values in the control plot for every canopy strata, except for the understory. Data on foliar C:N ratios for Amazonian leaves are limited. Fyllas et al. (2009) described a mean C:N ratio for leaves of ~23, similar to the ratio reported for the control plot in this study. Lower C:N ratios, without being associated with higher N values, correspond to thinner or less dense leaves (higher mass–area ratio), which are typical of shaded leaves, or perhaps is a mechanism to improve mesophyll conductance (Flexas et al. 2008). This degree of plasticity displayed by the Amazonian trees in this study, is perhaps the most unexpected result, as thicker leaves are associated with dry and sunny conditions.

Acknowledgements We thank P. Camargo, M. Moreira, F. Ishida, E. Mazzi, and our colleagues at the LBA-ECO and IPAM-Santarém offices. Financial support for this work was provided partially by a research grant from NASA LBA-Ecology to JRE, LBF, JAB and L.A.M.

Author contribution statement JRE, LAM and DCN designed the study and provided institutional support, TFD and JPHBO collected

and processed samples. LAM, JPHBP and TFD analysed the data and wrote the manuscript with contributions from all authors, DCN and PMB provided support to field activities, shared auxiliary data and scientific insights.

References

- Anderegg WRL, Flint A, Huang CY et al (2015) Tree mortality predicted from drought-induced vascular damage. *Nat Geosci* 8(5):367–371. <https://doi.org/10.1038/ngeo2400>
- Andreae MO, Rosenfeld D, Artaxo P et al (2004) Smoking rain clouds over the Amazon. *Science* 303(5662):1337–1342. <https://doi.org/10.1126/science.1092779>
- Blumenthal SA, Rothman JM, Chritz KL et al (2016) Stable isotopic variation in tropical forest plants for applications in primatology. *Am J Primatol* 78:1041–1054. <https://doi.org/10.1002/ajp.22488>
- Boisier JP, Ciais P, Ducharne A et al (2015) Projected strengthening of Amazonian dry season by constrained climate model simulations. *Nat Clim Chang* 5(7):656–660. <https://doi.org/10.1038/nclimate2658>
- Brando PM, Nepstad DC, Davidson EA et al (2008) Drought effects on litterfall, wood production and belowground carbon cycling in an Amazon forest: results of a throughfall reduction experiment. *Philos Trans R Soc B* 363:1839–1848. <https://doi.org/10.1098/rstb.2007.0031>
- Carswell FE, Meir P, Wandelli EV et al (2000) Photosynthetic capacity in a central Amazonian rain forest. *Tree Physiol* 20:179–186. <https://doi.org/10.1093/treephys/20.3.179>
- Cernusak LA, Winter K, Turner BL (2009) Physiological and isotopic ($\delta^{13}\text{C}$ and $\delta^{18}\text{O}$) responses of three tropical tree species to water and nutrient availability. *Plant Cell Environ* 32:1441–1455. <https://doi.org/10.1111/j.1365-3040.2009.02010.x>
- Cox P, Betts R, Collins M et al (2004) Amazonian forest dieback under climate-carbon cycle projections for the 21st century. *Theor Appl Climatol* 78:137–156. <https://doi.org/10.1007/s00704-004-0049-4>
- Cox PM, Pearson D, Booth BB et al (2013) Sensitivity of tropical carbon to climate change constrained by carbon dioxide variability. *Nature* 494(7437):341–344. <https://doi.org/10.1038/nature11882>
- Domingues TF, Martinelli LA, Ehleringer JR (2007) Ecophysiological traits of plant functional groups in forest and pasture ecosystems from eastern Amazonia, Brazil. *Plant Ecol* 193:101–112. <https://doi.org/10.1007/s11258-006-9251-z>
- Domingues TF, Martinelli LA, Ehleringer JR (2013) Seasonal patterns of leaf-level photosynthetic gas exchange in an eastern Amazonian rain forest. *Plant Ecol Divers* 7:189–203. <https://doi.org/10.1080/17550874.2012.748849>
- Duffy PB, Brando P, Asner GP, Field CB (2015) Projections of future meteorological drought and wet periods in the Amazon. *Proc Natl Acad Sci* 112(43):13172–13177. <https://doi.org/10.1073/pnas.1421010112>
- Farquhar GD, Werselaar R, Firth PM (1979) Ammonia volatilization from senescing leaves of maize. *Science* 203(4386):1257–1258. <https://doi.org/10.1126/science.203.4386.1257>
- Farquhar GD, Ehleringer JR, Hubick KT (1989) Carbon isotope discrimination and photosynthesis. *Annu Rev Plant Phys Plant Mol Biol* 40:503–537. <https://doi.org/10.1146/annurev.pp.40.06018.9.002443>
- Feldpausch TR, Phillips OL, Brienien RJW et al (2017) Amazon forest response to repeated droughts. *Glob Biogeochem Cycles* 30(7):964–982. <https://doi.org/10.1002/2015GB005133>

- Flexas J, Ribas-Carbó M, Diaz-Espejo A et al (2008) Mesophyll conductance to CO₂: current knowledge and future prospects. *Plant Cell Environ* 31:602–621. <https://doi.org/10.1111/J.1365-3040.2007.01757.X>
- Fyllas NM, Patiño S, Baker TR et al (2009) Basin-wide variations in foliar properties of Amazonian forest: phylogeny, soils and climate. *Biogeosciences* 6:2677–2708. <https://doi.org/10.5194/bg-6-2677-2009>
- Högberg P, Johnnison C, Högberg M et al (1995) Measurements of abundances of ¹⁵N and ¹³C as tools in retrospective studies of N balances and water stress in forests: a discussion of preliminary results. *Plant Soil* 168:125–133. <https://doi.org/10.1007/BF00029321>
- Huntingford C, Zelazowski P, Galbraith D et al (2013) Simulated resilience of tropical rainforests to CO₂-induced climate change. *Nat Geosci* 6(4):268–273. <https://doi.org/10.1038/ngeo1741>
- Marengo JA, Ambrizzi T, da Rocha H et al (2010) Future change of climate in South America in the late twenty-first century: intercomparison of scenarios from three regional climate models. *Clim Dyn* 35(6):1073–1097. <https://doi.org/10.1007/s00382-009-0721-6>
- McDowell N, Pockman WT, Allen CD et al (2008) Mechanisms of plant survival and mortality during drought: why do some plants survive while others succumb to drought? *New Phytol* 178:719–739. <https://doi.org/10.1111/j.1469-8137.2008.02436.x>
- Nardoto GB, Quesada CA, Patiño S et al (2014) Basin-wide variations in Amazon forest nitrogen-cycling characteristics as inferred from plant and soil ¹⁵N: ¹⁴N measurements. *Plant Ecol Divers* 7:173–187. <https://doi.org/10.1080/17550874.2013.807524>
- Nepstad DC, de Carvalho CR, Davidson EA et al (1994) The role of deep roots in the hydrological and carbon cycles of Amazonian forests and pastures. *Nature* 372(6507):666–669. <https://doi.org/10.1038/372666a0>
- Nepstad DC, Moutinho P, Dias-Filho MB et al (2002) The effects of partial throughfall exclusion on canopy processes, aboveground production, and biogeochemistry of an Amazon forest. *J Geophys Res* 107(D20):8085. <https://doi.org/10.1029/2001JD000360>
- Nepstad DC, Tohver IM, Ray D et al (2007) Mortality of large trees and lianas following experimental drought in an Amazon forest. *Ecology* 88:2259–2269. <https://doi.org/10.1890/06-1046.1>
- Norby RJ, De Kauwe MG, Domingues TF et al (2016) Model-data synthesis for the next generation of forest free-air CO₂ enrichment (FACE) experiments. *New Phytol* 209:17–28. <https://doi.org/10.1111/nph.13593>
- Oliveira RS, Dawson TE, Burgess SSO et al (2005) Hydraulic redistribution in three Amazonian trees. *Oecologia* 145:354–363. <https://doi.org/10.1007/s00442-005-0108-2>
- Ometto JPHB, Ehleringer JR, Domingues TF et al (2006) The stable carbon and nitrogen isotopic composition of vegetation in tropical forests of the Amazon Basin, Brazil. *Biogeochemistry* 79:251–274. <https://doi.org/10.1007/s10533-006-9008-8>
- Quesada CA, Lloyd J, Schwarz M et al (2010) Variations in chemical and physical properties of Amazon forest soils in relation to their genesis. *Biogeosciences* 7:1515–1541. <https://doi.org/10.5194/bg-7-1515-2010>
- Roberts P, Blumenthal SA, Dittus W et al (2017) Stable carbon, oxygen, and nitrogen, isotope analysis of plants from a South Asian tropical forest: implications for primatology. *Am J Primatol*. <https://doi.org/10.1002/ajp.22656>
- Rowland L, da Costa ACL, Galbraith DR et al (2015) Death from drought in tropical forests is triggered by hydraulics not carbon starvation. *Nature* 528(7580):119–122. <https://doi.org/10.1038/nature15539>
- Silva-Dias MAF, Rutledge S, Kabat P et al (2002) Cloud and rain processes in a biosphere–atmosphere interaction context in the Amazon Region. *J Geophys Res* 107(D20):8072. <https://doi.org/10.1029/2001JD000335>
- Sperry JS (2000) Hydraulic constraints on plant gas exchange. *Agric For Meteorol* 104(1):13–23. [https://doi.org/10.1016/S0168-1923\(00\)00144-1](https://doi.org/10.1016/S0168-1923(00)00144-1)